Thermou, G. E., Papanikolaou, V.K. & Kappos, A. J. (2014). Flexural behaviour of reinforced concrete jacketed columns under reversed cyclic loading. Engineering Structures, 76, pp. 270-282. doi: 10.1016/j.engstruct.2014.07.013

Flexural behaviour of reinforced concrete jacketed columns under reversed cyclic loading

Georgia E. Thermou[1,*], Vassilis K. Papanikolaou[1], Andreas J. Kappos[2]

[1] Civil Engineering Dept., Aristotle University of Thessaloniki, Thessaloniki, 54124, Greece

[2] Civil Engineering Dept., City University, EC1V 0HB London, UK

[*] Corresponding author, tel/fax: +30-2310-995466, e-mail: gthermou@civil.auth.gr

Abstract

The objective of the present study is the development of an analytical model for predicting the response under reversed cyclic loading of structural members with 'old-type' detailing, strengthened with reinforced concrete (RC) jacketing. The analytical model introduces one additional degree of freedom between the existing member (core of the retrofitted member) and its outer RC shell, thus allowing slip to take place at the interface between the existing member and the jacket. Shear resistance mechanisms, such as aggregate interlock, friction, and dowel action, are mobilized to resist slip. Existing constitutive models are further improved to describe the mechanisms that resist sliding under cyclic shear reversals and implemented for the first time in an analytical model for deriving the response of RC jacketed members. A calculation algorithm is developed to estimate the flexural response under cyclic loading taking into account slip at the interfaces. The sensitivity of the proposed analytical model to the shear transfer mechanisms degradation rules, as well as to the crack spacing estimation, was evaluated. The validity of the proposed analytical model is assessed against experimental results.

Keywords: Reinforced concrete; Shear resistance; Rehabilitation; Interface stress; Seismic design, Cyclic loading.

1. Introduction

Retrofitting of existing reinforced concrete (RC) structures is a sensitive issue in urban areas subjected to high seismic risk. A large portion of the current building inventory around the Mediterranean basin was built without any kind of seismic detailing since seismic design was not introduced at the time. In Greece, for example, a seismic code was first introduced in the late 1950s and RC walls were first used in multi-storey buildings in the 1960s. Therefore, strengthening the existing building stock seems to be the proper way to effectively reduce seismic risk; this entails the development of a retrofit strategy and the application of one or more local and/or global intervention techniques. Reinforced concrete jacketing is arguably the most appropriate intervention method for providing uniformly distributed lateral load capacity throughout the structure. Both stiffness and strength can increase substantially by the addition of the jacket, whereas proper design ensures a flexural plastic mechanism, preventing any brittle failure modes. Moreover, deformation capacity may also be enhanced through proper detailing of the strengthened member.

The effectiveness of the RC jacketing intervention method has been verified by studying the response of 44 specimens from 11 experimental studies [1-11], which constitute the experimental database of RC jacketed members compiled by the authors [12]. A key issue related to the response of the composite cross section is the interaction between the existing cross section and the outer shell (jacket). In an ideal situation, the construction of the jacket would ensure full composite action between the two bodies. Despite the fact that in some experimental studies this has been found to be feasible (e.g. [7, 11]), in real conditions (on the site) this seems not to be the case since slip takes place at the interface between the existing member and the jacket. In order to partially deal with this issue, apart from the surface preparation of the existing member, various means of connection between the 'old' cross section (which serves as the core of the jacketed member) and the jacket itself are adopted.

The response of members with composite cross section is largely influenced by the response characteristics of the most sensitive component, which, in the case of RC jacketed members, is considered to be the interface between the core and the jacket. The difficulty in tackling this complex problem of mechanics is that it is dominated by the shear resistance mechanisms mobilized due to sliding. A pragmatic design approach is adopted instead, which relies on the monolithic member approach for the analysis of composite members, making use of properly defined 'monolithicity factors' for obtaining the mechanical properties of the strengthened member. Design codes follow this approach by considering monolithicity factors based on empirical or semi-empirical relationships. In the case of Eurocode 8, Part 1.3 [13] and under the assumptions of: (i) full composite action between old and new concrete, (ii) application of full axial load on the jacketed member, and (iii) application of the concrete properties of the jacket over the full section of the element, monolithicity factors are equal to $K_V = 0.9$ for shear strength, $K_{My} = 1.0$ for yield moment , $K_{\theta u} = 1.0$ for the ultimate rotation, whereas for the yield rotation , the value $K_{\theta y} = 1.05$ applies when measures for roughening of the interface have been taken, and $K_{\theta y} = 1.20$ applies when measures other than roughening are taken for the connection of the jacket to the existing member or when no particular measures are taken. The Greek code for interventions [14] suggests monolithicity factors for shear strength $K_V = 0.9$, for stiffness, $K_K = 0.8$, and rotation at yield and ultimate $K_{\theta y} = 1.25$ and $K_{\theta u} = 0.80$, respectively.

Although some of the available models for predicting the behaviour between concrete interfaces under cyclic loading (e.g. [14]) have been implemented in computational models (finite element analysis) for estimating the response of RC jacketed members [15, 16], they have not been implemented in an analytical model. Such an analytical model is developed herein which takes into account slip at the interface between the core and the jacket and thus the shear transfer mechanisms mobilized along the contact interfaces. The model is capable of

predicting the flexural response of existing RC columns when RC jacketing is applied and considering that the longitudinal reinforcement placed in the jacket passes through holes drilled in the slab and new concrete is placed in the beam – column joint. The solution algorithm is based on previous research conducted by Thermou et al. [17] for monotonic loading. In this paper, it is further modified and extended to account for *cyclic* shear reversals. The sensitivity of the proposed analytical model to critical input parameters was evaluated and its validity was assessed through comparisons with experimental moment – curvature histories. A computer program was developed in-house, based on the proposed solution algorithm, which also comprises a useful tool for deriving monolithicity factors.

2. Interface resistance mechanisms under cyclic loading conditions

The addition of a new concrete layer (e.g. flexural strengthening of beams) or a new RC member (e.g. RC jacketing, RC infill walls) in various retrofit techniques entails issues related to the connection between existing and newly cast concrete. The response of the composite member, and subsequently of the whole structure, depends largely on the response characteristics of the interface, since shear transfer takes place. Describing in detail the mechanisms mobilized along interfaces due to slip and their interaction is a rather complex mechanical issue, especially under cyclic loading conditions where degradation should also be accounted for.

Aggregate interlock between contact surfaces, friction resulting from clamping action of reinforcement normal to the interface, as well as dowel action of any properly anchored reinforcement normal to the interface, are the mechanisms that resist sliding (slip). The contribution of the individual shear transfer mechanisms is given by:

$$\tau_{tot} = \tau_{agr} + \tau_f + \tau_D = \tau_{agr} + \mu\sigma_N + \tau_D \text{ ; where } \sigma_N = \sigma_c + \rho\sigma_s = \nu f_c + \rho\sigma_s \quad (1)$$

The first two terms in Eq. (1) collectively represent the *contribution of concrete* as they depend on the frictional resistance of the interface planes. In Eq. (1), τ_{agr} represents the shear resistance of the aggregate interlock mechanism, μ is the interface shear friction coefficient, σ_N is the normal clamping stress acting on the interface and τ_D is the shear stress resisted by dowel action in cracked reinforced concrete. The clamping stress represents any normal pressure, p, externally applied on the interface, but also the clamping action of reinforcement crossing the contact plane as illustrated in Fig. 1 (σ_s is the axial stress of the bars crossing the interface), ρ is the corresponding reinforcement area ratio, $v=N/(A_c f_c)=\sigma_c/f_c$ is the dimensionless axial load at the interface of A_c area, and f_c is the concrete compressive strength.

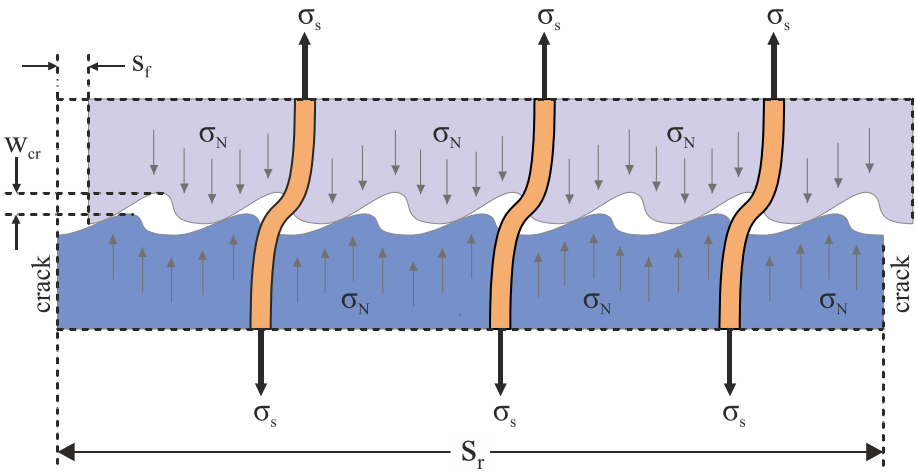

Figure 1: Slip at a concrete interface crossed by reinforcement.

2.1 Friction and dowel resistance

Shear transfer along interfaces has been a subject of research since the 1970s. Analytical models and design expressions, which are either empirical or based on substantial simplifications, have been proposed for the main shear transfer mechanisms (friction and dowel resistance) by considering that they act separately or jointly. Moreover, issues related to the influence of the roughness of the substrate surface, the differential shrinkage and stiffness of new-to-old concrete interfaces, as well as the compressive strength of the added concrete to an existing concrete substrate have been experimentally investigated [e.g. 18-22].

The models found in the literature can be classified into two categories. To the first belong those models where all forces are transferred through reinforcement [e.g. 23-25], whereas the second includes those models that, apart from reinforcement contribution, include a cohesion term [e.g. 26-32]. In the Modified Compression Field Theory (MCFT) [31] in the model of Tassios [32], by friction owing to clamping action of reinforcement normal to the interface. In the rest of the models, the cohesion term corresponds to the friction resistance developed along the interface.

In the present study, the cyclic behaviour of interfaces is described by the constitutive model developed by Vassilopoulou and Tassios [33] where the models of friction and dowel resistance of Tassios and Vintzileou [34], Vintzileou and Tassios [35, 36] are adopted. The interface model accounts for the combined shear force resistance mobilized along interfaces due to sliding both under monotonic and cyclic imposed deformations. This model was further modified by Palieraki *et al.* [37] and adopted by the current Greek code for interventions [KANEPE, 14]. It is used in this form in the present study, with additional modifications and extensions, as presented in the remainder of this section.

2.1.1 Constitutive law for friction resistance

The shear stress transferred through friction at the interface is described by the following set of equations [34]:

$$\frac{\tau_f(s)}{\tau_{f,u}} = 1.14\left(\frac{s}{s_u}\right)^{1/3} \quad \text{for } \frac{s}{s_u} \le 0.5 \tag{2a}$$

$$\frac{\tau_f(s)}{\tau_{f,u}} = 0.81 + 0.19\left(\frac{s}{s_u}\right) \quad \text{for } \frac{s}{s_u} > 0.5 \tag{2b}$$

where s_u is the higher value of slip attained (recommended value of 2 mm, in case of combination with dowels then s_u = 1 mm), whereas the peak value of friction resistance, τ_{fu}, is equal to:

$$\tau_{f,u} = \mu\left(f_c^2 \sigma_N\right)^{1/3} \tag{3}$$

where μ is the friction coefficient which, according to KANEPE [14], receives values equal to 0.4 and 0.6 for a smooth and a rough interface, respectively. Model code 2010 [38] suggests for concrete grades less than C50/60 representative mean values for the coefficient of friction, μ, equal to 0.5~0.7, 0.7~1.0 and 1.0~1.4 for smooth, rough (strongly roughened surface) and very rough interfaces, respectively. The value of $\tau_{f,u}$ (MPa) depends on the compressive strength of the weakest concrete of the interface, f_c, (typically f_c=$f_{c,old}$) [14]. In the experimental study conducted by Júlio *et al.* [20], it was found that the increase of the concrete compressive strength of the new layer compared to that of the existing one leads to an enhancement of the compressive strength of the interface, i.e. taking into account the compressive strength of the weakest concrete seems to be conservative. In order to take into account this experimental finding, Eq. (3) was modified here as follows:

$$\tau_{f,u} = 0.4 \cdot \beta\left(f_c^2 \sigma_N\right)^{1/3} = 0.4 \cdot \beta\left(f_c^2 \rho \cdot \sigma_s\right)^{1/3} = 0.4 \cdot \beta\left[f_c^2 \rho\left(\frac{0.3 s^{2/3} E_s f_c}{D_b}\right)^{1/2}\right]^{1/3} \tag{4}$$

where parameter β takes into account the increase of the higher value of friction resistance by means of the ratio of the compressive strengths of the new over the old concrete. Hence, β = 1.16 if $f_{c,new}/f_{c,old}$ = 1.0~1.36, β = 1.16~1.25 if $f_{c,new}/f_{c,old}$ = 1.36~2.75 and β = 1.25 if $f_{c,new}/f_{c,old} \geq$ 2.75. The term σ_N in Eq. (4) has been substituted by the term ($\rho \cdot \sigma_s$) (i.e. dimensionless axial load at the interface was considered, v=0, see Eq. (2), as in the case of the interface of RC jacketed members), where σ_s (MPa) is the steel bar stress at the contact plane which for uniform bond stresses along the embedment length is equal to $(0.3 s^{2/3} E_s f_{c,old}/D_b)^{1/2}$

according to Vassilopoulou and Tassios [30]. E_s (MPa) is the elastic modulus of steel and D_b (mm) is the dowel diameter (stirrup diameter of the jacket in the case of the proposed model).

According to the degradation rule proposed by Palieraki *et al.* [37] and adopted by the Greek code for interventions [14] the frictional resistance is reduced at each cycle, n, according to (see Fig. 2(a)):

$$\tau_{f,n} = \tau_{f,1} \cdot \tau_{deg} = \tau_{f,1}\left\{1 - \left[0.05(n-1)^{1/2}\left(\frac{f_c}{\sigma_N}\right)^{1/2}\left(\frac{s}{s_u}\right)^{1/3}\right]\right\} \tag{5}$$

where $\tau_{f,1}$ is the peak frictional resistance value attained in the first cycle.

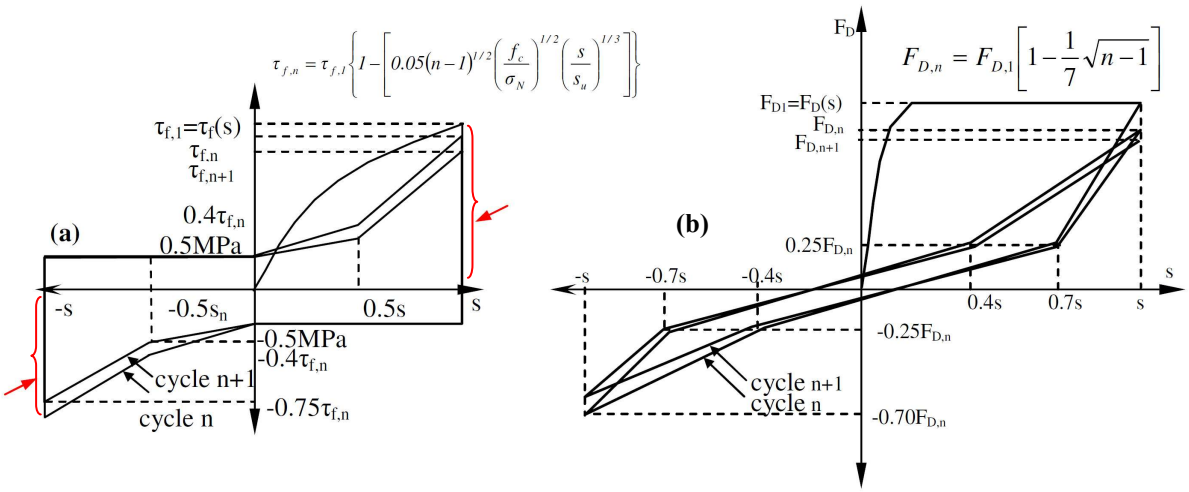

Figure 2. Response to symmetric cyclic loading: (a) friction and (b) dowel.

2.1.2 Constitutive law for dowel resistance

In the dowel model proposed by Vintzileou and Tassios [35, 36], the bar behaves similarly to a horizontally loaded free-headed pile embedded in cohesive soil, and yielding of the dowel and crushing of concrete occur simultaneously. Dowel force, F_D, is given as a function of slip, s, by:

$$\frac{F_D(s)}{F_{D,u}} = 0.5\frac{s}{s_{el}} \text{ for } s \le s_{el} = 0.006\,D_b \tag{6a}$$

$$s = 0.006 D_b + 1.76 s_u \left[\left(\frac{F_D(s)}{F_{D,u}} \right)^4 - 0.5 \left(\frac{F_D(s)}{F_{D,u}} \right)^3 \right] \text{ for } \frac{F_D(s)}{F_{D,u}} \geq 0.5 \quad (6b)$$

where s_{el} (mm) is the elastic slip value, s_u (mm) is the ultimate slip value, $F_{D,u}$ (N) is the ultimate dowel force and D_b (mm) is the diameter of the dowels (the legs of the jacket transverse reinforcement if no additional dowels are provided). The ultimate dowel strength and associated interface slip are given by:

$$F_{D,u} = 1.3 D_b^2 \left(f_{cd} f_{yd} \right)^{1/2}; \quad s_u = 0.05 D_b \quad (7)$$

where f_{yd} (= f_y/1.15 MPa) is the design yield strength of steel and f_{cd} (= f_{ck}/1.5 MPa) is the design concrete compressive strength. The degradation rule adopted by KANEPE [14] is (Fig. 2(b)):

$$F_{D,n} = F_{D,1} \cdot D_{deg} = F_{D,1} \left[1 - \frac{1}{7} \sqrt{n-1} \right] \quad (8)$$

where $F_{D,1}$ (N) is the peak dowel resistance attained in the first cycle and n the number of cycles.

2.2. Modifications to the interface constitutive laws

The friction and dowel resistance models presented in the previous section were further enhanced to account for the case of *non-symmetric reversed cyclic loading* that is typical in seismic situations. The new modifications in the above dowel and friction constitutive models are:

i. Since the dowel and friction response shapes in Fig. 3 are non-symmetrical, they are applicable only for an initial positive slip step. Consequently, if the initial step involves negative slip, the response shapes should be mirrored, hence a global 'direction' factor $\lambda = \text{sign}(s)$ is defined when the absolute current slip value exceeds the dowel elastic slip limit $s_{el} = 0.006 \cdot D_b$ for the first time.

ii. In the case of unloading or reloading from the envelope curve, the attained slip (s) and response (τ_f or F_D), at the instance of slip reversal, are stored. At the same instance, the absolute maximum recorded slip value throughout the loading history (s_{max}) is also stored.

iii. Upon any slip reversal, the applicable range of cyclic response is updated using Eqs. (9) and (10) for friction and dowel forces, respectively. Fig. 4 depicts the corresponding unloading and reloading paths for the dowel model. In the special case when the starting (s_s) and ending (s_n) slip values are of the same sign, the depicted trilinear path is reduced to a straight line. Furthermore, in order to improve numerical stability, the vertical drops in friction force (arrows in Fig. 2a) were mitigated with a slip reduction of 10 %.

$$\begin{array}{ll} \text{friction range} & (s_s,\ \tau_{f,s}) \sim (s_n,\ \tau_{f,n}) \\ \text{unloading} & s_n = -s_{max},\ s_s > 0 : \tau_{f,n} = -0.75 \cdot |\tau_{f,s}| \ \textit{and}\ s_s < 0 : \tau_{f,n} = -|\ \tau_{f,s}\ | \\ \text{reloading} & s_n = s_{max},\ s_s > 0 : \tau_{f,n} = -|\tau_s| \ \text{and}\ s_s < 0 : \tau_{f,n} = -|\ \tau_{f,s}\ | \ / \ 0.75 \end{array} \quad (9)$$

$$\begin{array}{ll} \text{dowel range} & (s_s,\ F_{D,s}) \sim (s_n,\ F_{D,n}) \\ \text{unloading} & s_n = -s_{max},\ s_s > 0 : F_{D,n} = -0.7 \cdot |\ F_{D,s}| \ \textit{and}\ s_s < 0 : F_{D,n} = -|\ F_{D,s}| \\ \text{reloading} & s_n = s_{max},\ s_s > 0 : F_{D,n} = -|F_{D,s}| \ \textit{and}\ s_s < 0 : F_{D,n} = -|\ F_{D,s}| \ / \ 0.7 \end{array} \quad (10)$$

If the current peak slip value (s_n) is exceeded during loading (i.e. its absolute value is larger than s_{max}), the loading path continues on the envelope curve.

i. In the case of $|s| < s_{el}$, elastic response is considered and no cyclic rules are applied.

ii. The final element of the extended and improved cyclic interface model is the introduction of two force degradation factors for dowel and friction models. These degradation factors operate on the envelope curves and reflect the force degradation due to cyclic loading. In the original suggestion by Vassilopoulou and Tassios [33] and in the later amendments of the Greek code for interventions [14], strength degradation depends on the number of symmetric cycles (n). In order to extend this concept to arbitrary loading history, an equivalent number of cycles (n_{eq}) is introduced herein, which depends on the cumulative slip (Σs):

$$n_{eq} = \frac{1}{4}\left(\frac{\sum s}{|s_{max}|} + 1\right) \tag{11}$$

and the degradation factors for friction (τ_{deg}) and dowel (D_{deg}) actions are updated as follows:

$$\tau_{deg} = 1 - \alpha \cdot 0.05 \cdot \sqrt{\frac{\sum s/|s_{max}| + 1}{4}} \cdot \left(\frac{f_c}{\sigma_c}\right)^{1/2} \left(\frac{|s_{max}|}{s_u}\right)^{1/3} \tag{12}$$

$$D_{deg} = 1 - \alpha \cdot \frac{1}{7}\sqrt{\frac{\sum s/|s_{max}| + 1}{4}} \tag{13}$$

where coefficient α is the degradation parameter.

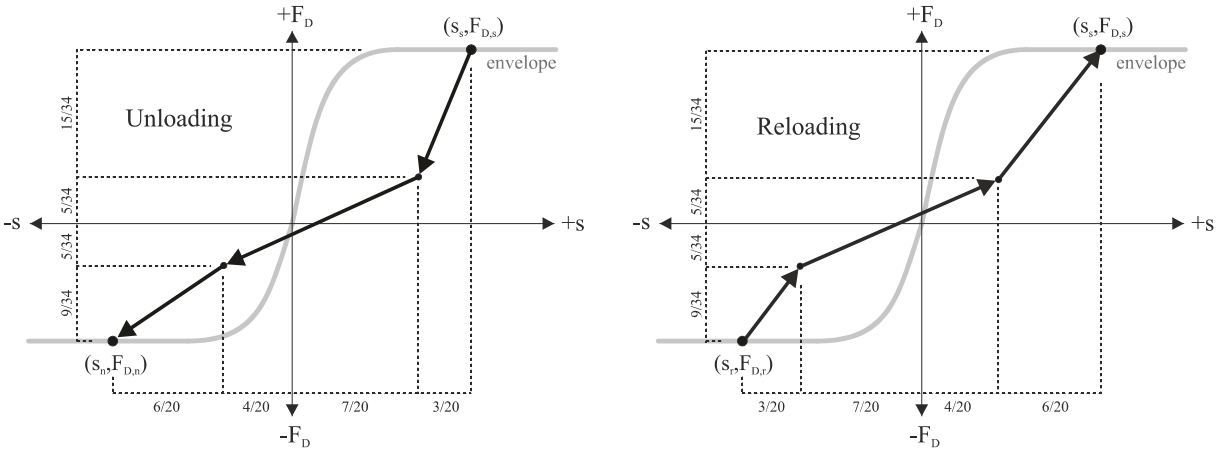

Figure 3. Unloading and reloading paths for dowel action.

The above degradation factors are pre-calculated at the instance of reloading, yet finally applied on the envelope curves at the end of the cycling procedure, i.e. when the peak slip value (s_n) is exceeded and the loading path continues on an updated envelope curve. The transition between the former and the updated envelope is performed on the final branch of the cyclic load path, as depicted in Fig. 4 for the dowel model.

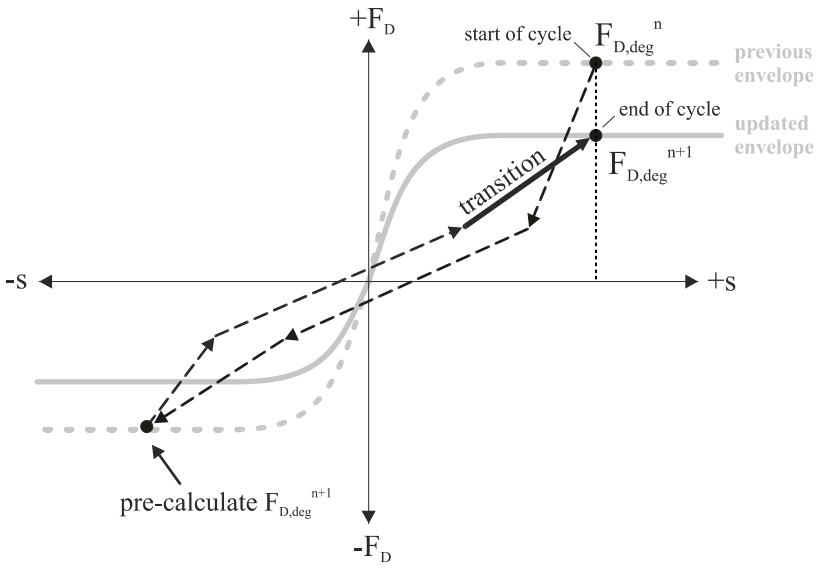

Figure 4. Calculation and update of the degradation factor and envelopes.

3. Analytical model for RC jacketed members under cyclic loading conditions

In the case of composite cross sections where an outer shell is placed around the core of the cross section, the relative slip between the two bodies depends largely on their interconnection. In one extreme case the jacket could slip relative to the core without mobilizing any kind of shear resistance, which is the case of zero friction. One of the other possible scenarios (suggested by experimental evidence) is when cracks form parallel to the interfaces between the two external layers which represent the contribution of the jacket and the internal one which represents both the core (existing cross section) and the web of the jacket shell [4-6, 9]. Thus, two sliding planes are created as shown in Fig. 5. Slip at the sliding plane mobilizes the shear transfer mechanisms such as aggregate interlock, friction owing to clamping action, and dowel action of the stirrup legs of the jacket and the dowels placed at the interface whenever this is introduced as an additional connection measure (Fig. 5).

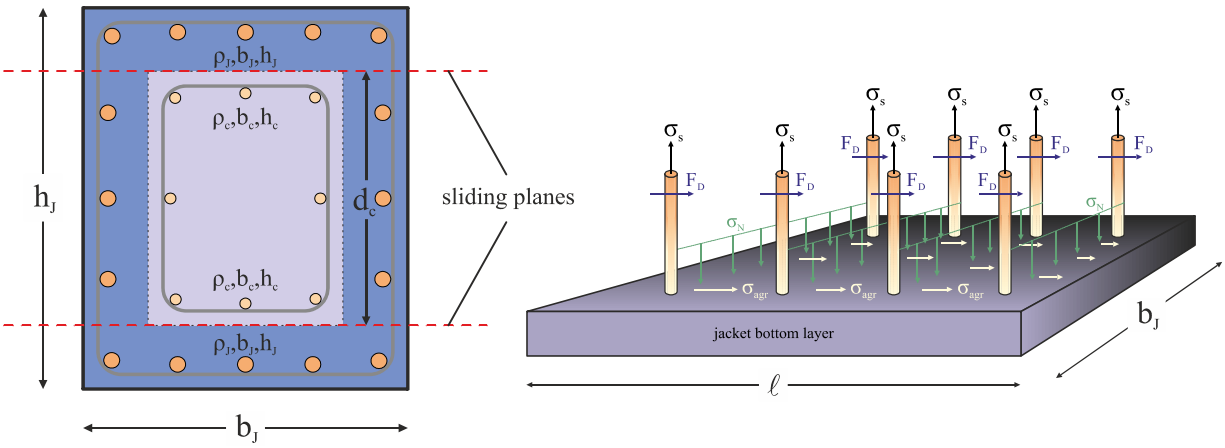

Figure 5. Definition of sliding planes; Shear transfer mechanisms at the interface between the jacket and the core.

The proposed analytical model for predicting the flexural response of RC members strengthened with concrete jackets under cyclic loading conditions considers that slip takes place along the interfaces between the existing member and the jacket. Relative slip at the interface between the existing member and the jacket is introduced following the same conceptual framework developed by Thermou et al. [17]. The model is extended here to cyclic loading conditions after performing a series of adaptations and additions. The proposed analytical model introduces a degree of freedom allowing the relative slip at the interface between the existing member and the jacket. Slip along the member length is attributed to the difference in normal strains at the contact interfaces (Fig. 6). For flexural analysis, the cross section is divided into three layers which deform with the same curvature, φ (Fig. 6). It is recalled that the two external layers represent the contribution of the jacket, whereas the internal one represents both the core (existing cross section) and the web of the jacket shell. The difference in normal strain at the interface between layers (Fig. 6, bottom interface: ε_{j3}-ε_{c2}; top interface: ε_{c1}-ε_{j2}) accounts for the corresponding slip in the longitudinal direction (x-axis in Fig. 6). Along the vertical plane (i.e. on faces normal to the z-axis, Fig. 6), the resultant forces are nearly zero for the case that the jacket longitudinal tension reinforcement is evenly distributed along the perimeter (as in the RC jacketed cross section shown in Fig. 6). The vertical slice of the jacketed cross section is almost self-equilibrating (the rectangular

portion of the cross section of thickness t_J, to the left of line A-A′ in Fig. 6), since the compression and tension forces over the height of the segment are almost equal, thus resulting in a total stress resultant close to zero.

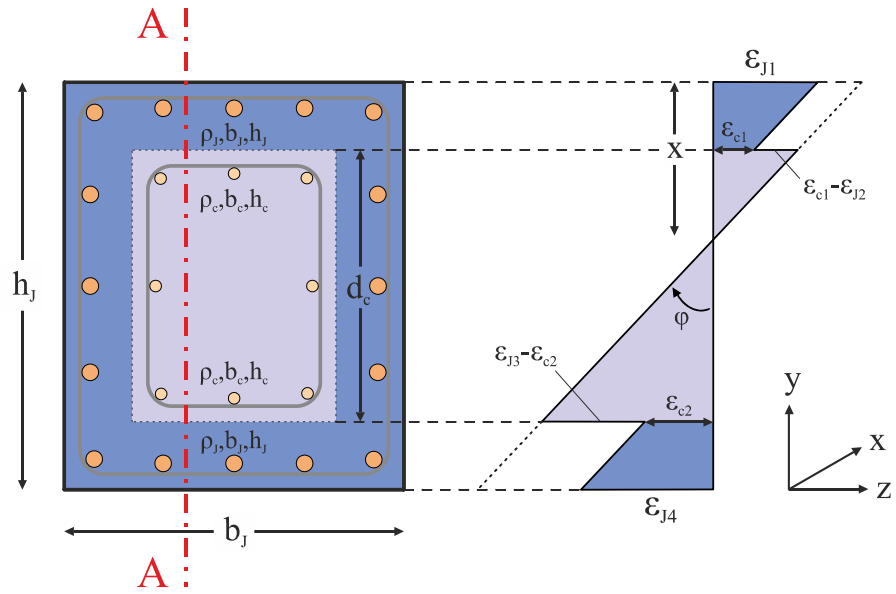

Figure 6. Strain profile of the jacketed cross section. (πρέπει να διορθωθεί η κατακόρυφη διακεκομμένη και να πάει λίγο πιο αριστερά στο όριο της κατακόρυφης διεπιφάνειας – **to be done)**

When concrete dries out at the perimeter of the jacket, it tends to contract, thereby producing tensile forces perpendicular to the interface, leading eventually to cracking of concrete. The effect of differential shrinkage on the design of composite concrete members has been investigated by various researchers [e.g. 22, 39]. Lampropoulos and Dritsos [15, 16] studied the effect of shrinkage on the response of RC jacketed columns by developing a computational (finite element) model for the behaviour of reinforced concrete columns subjected to monotonic and cyclic loading. It was demonstrated that concrete shrinkage induces slip at the interface between the old and the new concrete as well as tensile stresses in the jacket concrete. The presence of shrinkage creates a biaxial stress state for the concrete. In the analytical model proposed herein, differential shrinkage was ignored, assuming for simplicity that the RC jacketed cross section is subjected to uniaxial stress state. It would have been possible to indirectly take into account the effect of differential shrinkage utilizing the

proposed model by introducing a reduced value for the concrete compressive strength. It is noted that estimating the level of reduction is very difficult considering the complexity of the mechanism. Moreover, the shrinkage effect depends on the age of concrete and the environmental conditions (ambient humidity), which further complicate the treatment of the shrinkage effect.

3.1 Crack spacing estimation and shear stress demand at the interfaces

In RC members, the estimation of the crack spacing is related to the transfer of the bond stress at the tension zone of the member (e.g. [38]). In the proposed analytical model the bottom layer of the additional layer of concrete and reinforcement is treated as a composite type of reinforcement for the existing cross section. Following the concept developed by Thermou et al. [17], shear transfer at the interface between the existing member and the jacket is carried out between half crack intervals along the length of the jacketed member as also done in bond analysis. The distance between those cracks, taken as s_r, is a key element of the proposed analytical model. It is assumed that cracks are equally distributed at distance s_r along the member's length. This implies that stabilization of cracks has occurred in the jacket. At this stage the jacket steel stress at the crack, $\sigma_{s,cr}^{J}$ exceeds the limit [38]:

$$\sigma_{s,cr}^{J} > f_{ctm}^{J} \frac{1+\eta\rho_{s,eff}^{J}}{\rho_{s,eff}^{J}} \tag{14}$$

where f_{ctm}^{J} (MPa) is the tensile strength of concrete of the jacket, η (=E_s/E_{cm}) is the modular ratio and $\rho_{s,eff}$ is the effective reinforcement ratio defined as the total steel area divided by the area of mobilized concrete in tension [38]. Using the same considerations in the combined section it may be shown that a number of the external cracks penetrate the second layer (core) of the jacketed member (Fig. 7).

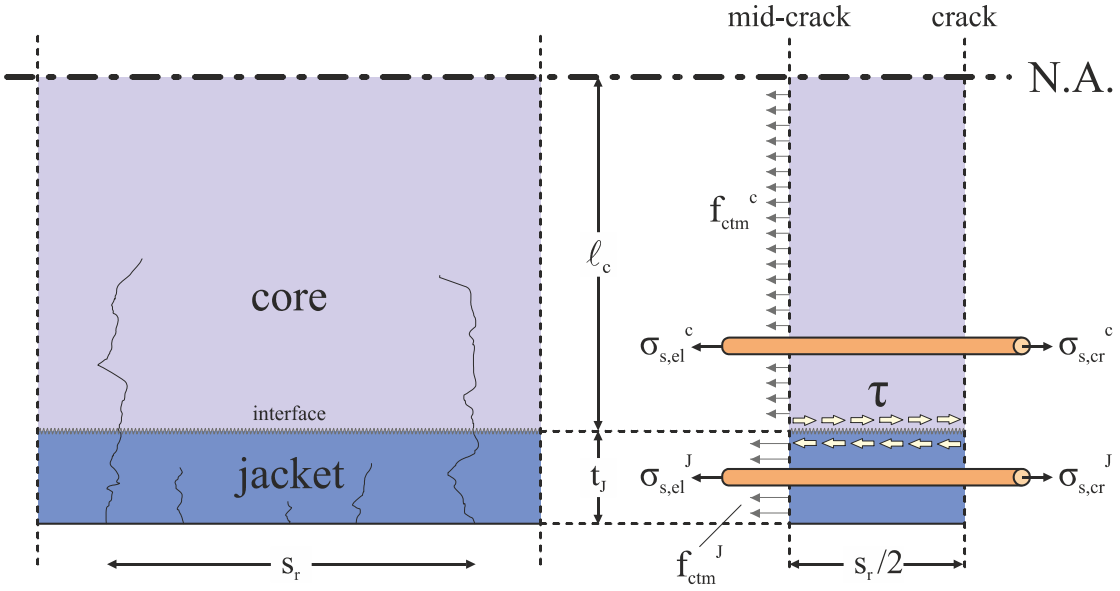

Figure 7: Crack spacing, s_r, and free body equilibrium in the tension zone of the composite section.

- **Crack spacing estimation**

The crack spacing, s_r, may be estimated after crack stabilization and assuming that the neutral axis depth is almost constant in adjacent cross sections. The free body equilibrium in the tension zone of the composite cross section is depicted in Fig. 7. From the equilibrium of the bottom layer of the jacket, the shear stress developed at the interface, τ, is equal to:

$$\tau \cdot \frac{s_r}{2} \cdot b_J + f_{ctm,J} t_J b_J = n_J \frac{\pi D_{b,J}^2}{4} \left(\sigma_{s,cr}^J - \sigma_{s,el}^J \right) \Rightarrow \tau \cdot \frac{s_r}{2} \cdot b_J = n_J \pi D_{b,J} f_{b,J} \cdot \frac{s_r}{2} - f_{ctm,J} t_J b_J \Rightarrow$$
$$\tau = n_J \frac{\pi D_{b,J} f_{b,J}}{b_J} - \frac{2}{s_r} f_{ctm,J} t_J \qquad (15)$$

The equilibrium of the core of the composite section in tension yields:

$$2 f_{ctm,J} \ell_c t_J + f_{ctm,c} \ell_c b_c - n_c \frac{\pi D_b^2}{4} \left(\sigma_{s,cr}^c - \sigma_{s,el}^c \right) = \tau \cdot \frac{s_r}{2} \cdot b_J \Rightarrow$$
$$2 f_{ctm,J} \ell_c t_J + f_{ctm,c} \ell_c b_c - n_c \pi D_{b,c} f_{b,c} \cdot \frac{s_r}{2} = \tau \cdot \frac{s_r}{2} \cdot b_J \Rightarrow \qquad (16)$$
$$s_r = 2 \frac{\left(2 f_{ctm,J} \ell_c t_J + f_{ctm,c} \ell_c b_c \right)}{n_c \pi D_{b,c} f_{b,c} + \tau b_J}$$

After substitution of Eq. (16) in Eq. (15), the expression for estimating the crack spacing, s_r, is defined as:

$$s_r = \frac{2}{\pi} \frac{\left[f_{ctm,c} \ell_c b_c + f_{ctm,J} t_J \left(2\ell_c + b_J \right) \right]}{\left(n_J D_{b,J} f_{b,J} + n_c D_{b,c} f_{b,c} \right)} \tag{17}$$

where b_c, b_J (mm) is the width of the core and the jacketed cross section, respectively, ℓ_c (mm) is the height of the tension zone in the core component of the composite cross section, $f_{ctm,c}$, $f_{ctm,J}$ (MPa) are the tensile strength of the concrete core and the jacket, respectively, n_c, n_J are the number of bars in the tension steel layer of the core and the jacket, respectively, $D_{b,c}$, $D_{b,J}$ (mm) are the bar diameter of the core and jacket longitudinal reinforcement, respectively, and $f_{b,c}$, $f_{b,J}$ (MPa) are the average bond stress of the core and the jacket reinforcement layer, respectively. An upper and a lower limit value of the area mobilized in tension could be defined depending on the definition of ℓ_c as follows:

$$2.5\left(c_c + D_{b,w} + D_{b,c}/2 \right) \le \ell_c \le \left(h_J - x - t_J \right) \tag{18}$$

where c_c (mm) is the concrete cover of the core, $D_{b,w}$, $D_{b,c}$ (mm) are the bar diameter of the core stirrups and core longitudinal reinforcement, h_J (mm) is the height of the jacketed cross section, x (mm) is the height of the compressive zone of the composite cross section (Fig. 5) and t_J (mm) is the thickness of the jacket. The lower value of ℓ_c (mm) corresponds to the mobilized area in tension prescribed by the Model Code 2010 [38]; the highest value of ℓ_c is shown in Fig. 7.

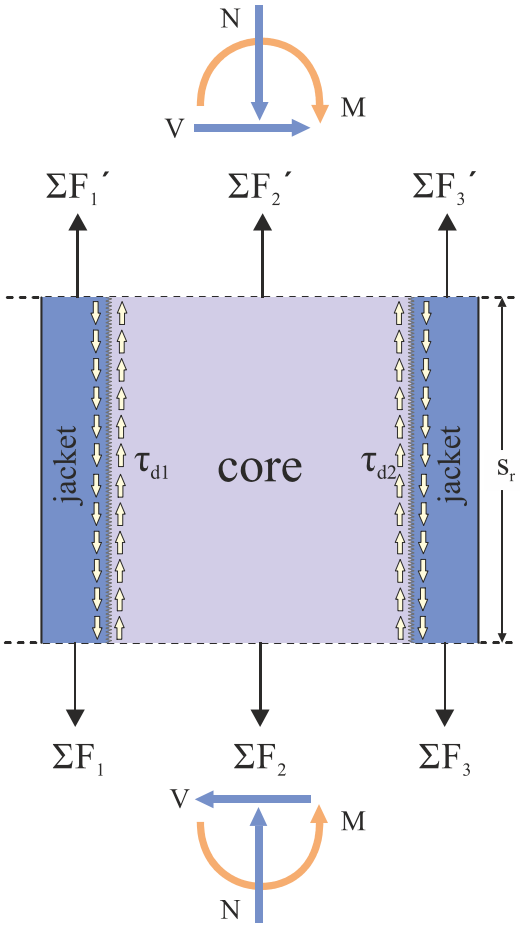

Figure 8: Section equilibrium between adjacent cracks.

- **Shear stress demand**

Shear stress demand at the interfaces, $\tau_{d,i}$, is determined by examining the cross section along the height and at a member length equal to the distance between successive cracks (Fig. 8). The layer force resultant ΣF_i (sum of concrete and steel forces at each layer), for the externally applied axial load, N_{ext}, is used to calculate the vertical shear stress demand in the member, $\tau_{d,i}$. It is noted that there is no stress state in the existing column due to dead load before the axial load is applied. With the assumption that reversal of the shear flow, q, takes place at a length equal to $s_r/2$ the average stress demand $\tau_{d,i}$ is equal to:

$$\tau_{d,i} = \frac{\Sigma F_i}{0.5\, s_r\, b_J} \tag{19}$$

where ΣF_i is the layer force resultant of the bottom and top layer equal to the jacket thickness t_J, b_J is the width of the jacketed cross section, and s_r is the crack spacing length.

3.2 Algorithm for calculating moment – curvature histories

The algorithm proposed herein calculates the moment – curvature histories of RC members retrofitted with RC jackets, taking into account interface slip between the existing member (core) and the jacket, under cyclic loading conditions. In particular, given a curvature 'loading' history, the objective at each loading step is twofold: (i) to establish equilibrium between shear stress capacity and demand at the interfaces for relative slip (s_r) and, at the same time, (ii) to establish force equilibrium along the entire cross section. Apart from the previously presented cyclic interface model to simulate the slip effect between the core (old) and jacket (new) concrete, two cyclic constitutive models for concrete and steel materials are required for setting up a fibre representation of the jacketed RC section. The constitutive model for concrete implemented in the present study is based on the uniaxial stress-strain relationship suggested by Mander et al. [40], as adapted by Martinez-Rueda and Elnashai [41]. The confinement action due to transverse reinforcement is captured by a passive confinement factor (K), which is considered constant during loading. For reinforcing steel, the cyclic constitutive model by Menegotto and Pinto [42] incorporating the isotropic hardening rules by Filippou et al. [43] was implemented. To avoid further complicating the analytical model, perfect bond was considered between steel bars and concrete. Moreover, preloading of the existing column was ignored. In most practical applications, the core is under stress prior to applying the jacket. The effect of preloading has been studied both experimentally and analytically. Test results are rather controversial, since there are researches who claim that preloading should be considered and it has a favourable effect [5], whereas others claim that preloading has no noticeable influence on test results [7, 11]. Analytical investigation on

preloading has shown that for reasonable column axial compression levels the effect of core preloading can be safely ignored [44].

The computational procedure is based on the classic fibre decomposition approach due to the non-cylindrical stress field (non-uniform in one direction) emanating from the load path dependency that characterizes cyclic loading [45]. Within this framework, the section is divided into a fine fibre mesh (Fig. 9(a)) and each fibre is associated with the corresponding cyclic material constitutive model. It is noted here that three distinct confinement regions are defined for the jacketed section (unconfined, partially confined and fully confined), each associated with a properly calculated confinement factor according to the confinement model suggested by Kappos [46]. For the stress integration of the section internal forces, following the Bernoulli-Euler assumption (i.e. plane sections remain plane and perpendicular to the axis of the column), the complete strain profile is described through four distinct parameters (φ, ε_o, ε_A, ε_B), in order to account for possible interface slip, as depicted in Figure 9(b).

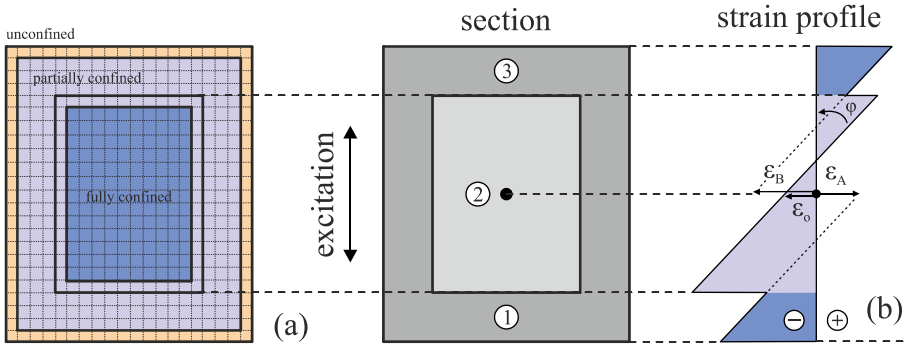

Figure 9: (a) Fibre decomposition (half of the section is discretised due to simple symmetry); (b) Strain profile – definition of parameters φ, ε_o, ε_A, ε_B.

For each curvature step ($\Delta\varphi$), the goal is to calculate the bending moment (M) corresponding to the new curvature value $\varphi+\Delta\varphi$, for a given constant external axial load (N_{ext}). This procedure is repeated for the entire curvature history, in order to finally produce the cyclic moment-curvature response curve. Hence, for each (predefined) curvature step, in order

to satisfy the aforementioned equilibrium conditions, the three unknowns ($\Delta\varepsilon_o$, $\Delta\varepsilon_A$, $\Delta\varepsilon_B$) together with the predefined $\Delta\varphi$, which define the section strain profile, should be determined. Shear strength capacity of the top and bottom interface, τ_1 and τ_2, are estimated from the respective slip values, s_1 and s_2, according to the constitutive law that describes the behaviour of the interface under cyclic loading (Eqs. 2-9). The incremental change of the strain profile described above ($\Delta\varphi$, $\Delta\varepsilon_o$, $\Delta\varepsilon_A$, $\Delta\varepsilon_B$) causes slip on the top and bottom interface equal to:

$$\Delta s_1 = \left(\Delta\varepsilon_B - \Delta\varepsilon_o\right)\frac{s_r}{2} \rightarrow \text{top interface} \; ; \; \Delta s_2 = \left(\Delta\varepsilon_A - \Delta\varepsilon_o\right)\frac{s_r}{2} \rightarrow \text{bottom interface} \tag{20}$$

Shear strength demand at the upper and bottom interface, $\tau_{d,1}$ and $\tau_{d,2}$, is also estimated according to Eq. (19). Next, the stresses are integrated and the layer force resultant ΣF_i is calculated (Fig. 8). In the final step the simultaneous equilibrium of the interfaces and the cross section is checked. Since the response of the cyclic constitutive models is load-path dependent, a 'trial-and-error' approach attempting different combinations of the three unknown values until convergence is required. To this purpose, an evolutionary algorithm is applied, specifically the differential evolution approach [47], which is an established metaheuristic method that optimizes a problem by iteratively improving a candidate solution (i.e. the present set of unknowns $\Delta\varepsilon_o$, $\Delta\varepsilon_A$, $\Delta\varepsilon_B$) with regard to a given measure of quality, called the objective function. The objective function selected herein is the out-of-balance forces developed in the section. In case of convergence the moment resultant (M) is calculated and stored together with the corresponding curvature value (φ). The procedure is repeated for the entire curvature history. Calculations stop when the shear capacity of the interface is exceeded.

4. Sensitivity analysis of the proposed analytical model

From the procedure described in the previous section it is evident that many parameters come into play in the proposed analytical solution algorithm for RC jacketed columns that may influence substantially the obtained results. The most crucial one seems to be the crack spacing since it strongly influences the value of the shear demand at the interface, $\tau_{d,i}$, and thus controls the overall response of the member (Eq. 20). Moreover, the cyclic nature of the loading and the degradation rules adopted for both construction materials, as well as the shear resistance mechanisms, all affect the overall response. In the present study, the constitutive laws of friction and dowel resistance (presented in section 2) are implemented for the first time to analyse the response of a composite cross section such as that of the RC jacketed structural member. The impact of the degradation parameter α used for the estimation of the degradation factors for friction (τ_{deg}) and dowel (D_{deg}) actions (Eqs. 12 and 13) on the derived moment –curvature histories is also studied.

4.1 Influence of crack spacing

The crack spacing is estimated according to Eq. (17) based on the premise that shear transfer at the interface between the existing member and the jacket is carried out between half crack intervals along the length of the jacketed member as customarily done in bond analysis. Apart from the height of the tension zone in the core component of the composite cross section, ℓ_c, which in itself constitutes a parameter for further investigation, the average bond stress of the core and the jacket reinforcement layer $f_{b,c}$, $f_{b,J}$, influence significantly the estimated value of the crack spacing. The expressions provided by Eurocode 2 [48] and *fib* Model Code [38] are utilised for the definition of the average bond strength as follows:

According to Eurocode 2 [48],

$$f_b = 2.25 \cdot \eta_1 \cdot \eta_2 \cdot f_{ctm} \tag{21}$$

where f_{ctm} (=$0.3f_c^{2/3}$) is the concrete tensile strength (mean value), η_1 is the coefficient related to the quality of bond and the position of the bar during concreting, taken equal to 1 for good bond conditions, and η_2 is related to the bar diameter, taken equal to 1 for $D_b < 32$ mm. It is noted that there is no provision for the case of plain longitudinal bars. In that case, f_b was taken equal to f_{ctm} following the guidelines of the Greek Seismic Code [49].

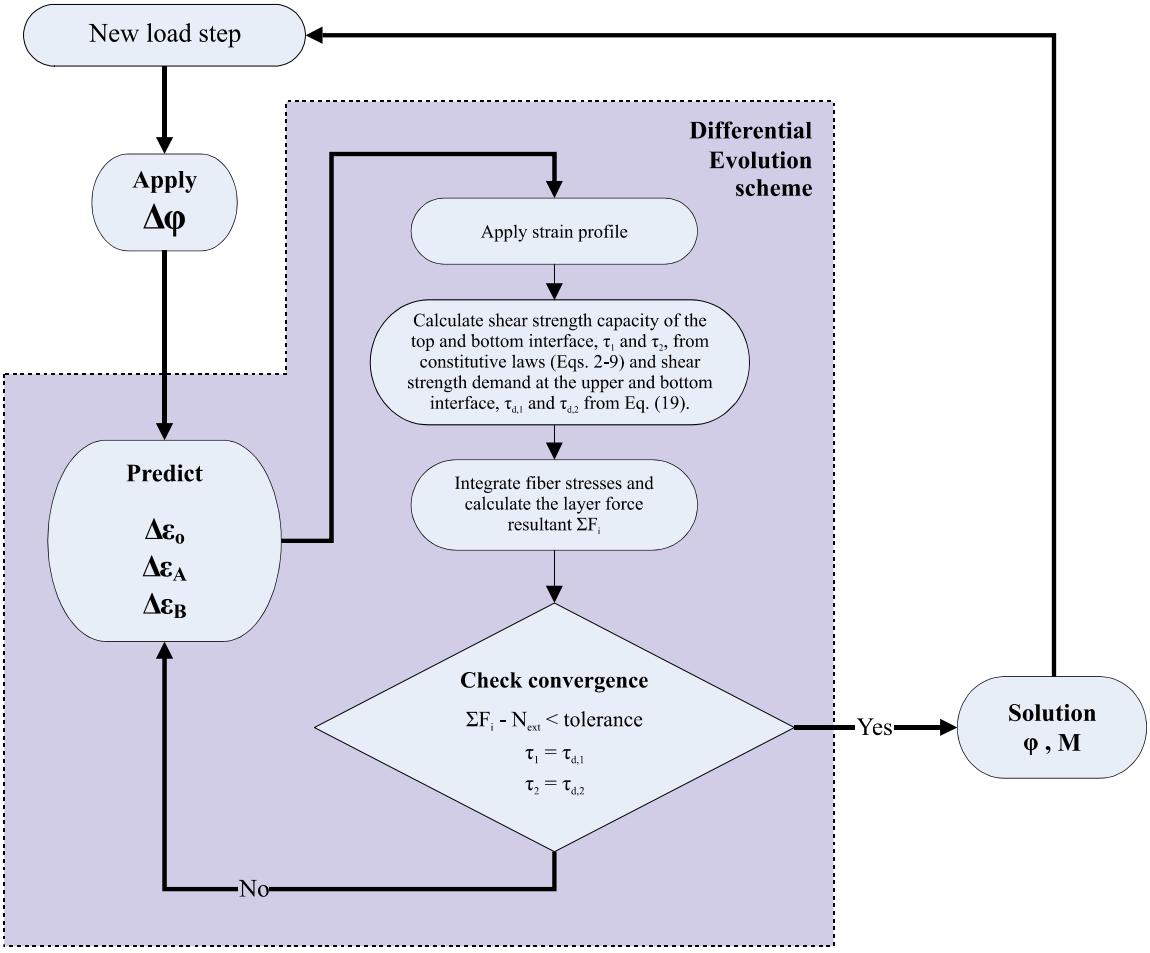

Figure 10: Flowchart of the solution algorithm.

The *fib* Model Code 2010 [38] provides the following expression:

$$f_b = (\alpha_2 + \alpha_3) f_{b,o} + 2\,p_{tr} < 2\,f_{b,o} + 0.4\,p_{tr} < 2.5\sqrt{f_c} \tag{22}$$

where p_{tr} (MPa) is the mean compression stress perpendicular to the potential splitting failure surface at the ultimate limit state, α_2 and α_3 account for the influence of passive confinement from cover and from transverse reinforcement, respectively, in excess of their respective permissible minima, given by:

$$\alpha_2 = \left(c_{min}/D_b\right)^{0.5} \cdot \left(c_{max}/c_{min}\right)^{0.15} \rightarrow for\ ribbed\ bars\ \ ;\ \alpha_2 = 1 \rightarrow for\ plain\ bars \tag{23a}$$

$$\alpha_3 = k \cdot n_1 \cdot A_{sv}/\left(n_b \cdot D_b \cdot s_v\right) \tag{23b}$$

c_{min}, c_{max} (mm) refer to the minimum and maximum concrete cover, D_b (mm) is the bar diameter, k is an effectiveness factor dependent on the reinforcement detail taken for the needs of the present study equal to $k = 15$, n_1 is the number of legs of confining reinforcement at a section, A_{sv} is the cross sectional area (mm^2) of one leg of a confining bar, s_v is the longitudinal spacing (mm) of confining reinforcement, n_b is the number of anchored bar or of the smaller of a pair of lap-spliced bars (mm). The term $f_{b,o}$ (MPa) corresponds to the basic bond length defined as:

$$f_{b,o} = \eta_1 \cdot \eta_2 \cdot \eta_3 \cdot \eta_4 \left(f_c/20\right)^{0.5} \tag{24}$$

where η_1 is equal to 1.8 and 0.9 for ribbed and plain bars, respectively, η_2 is equal to 1 for good bond conditions, η_3 is equal to 1 for $D_b < 20$ mm, and η_4 is equal to 1 for $f_{yk} = 500$ MPa, 1.2 for $f_{yk} = 400$ MPa, 0.85 for $f_{yk} = 600$ MPa and f_c is the concrete compressive strength.

The role of crack spacing on the response was examined for specimen QRC from the experimental campaign of Boussias et al. [9]. Specimen QRC has a 250 mm square cross section where a 75 mm thickness jacket is added, resulting in a shear span $L_s = 1.6$ m. No special measures were taken to connect the jacket to the existing cross section (core). This implies that a natural surface was considered, thus minimizing the parameters that may affect the response of the jacketed member and rendering it suitable for carrying out this sensitivity study. The original cross section comprises plain longitudinal and transverse bars, whereas ribbed bars are used as longitudinal and transverse reinforcement in the jacket. Details

regarding the reinforcement detailing and material properties are summarised in Table 1. Eqs. (21) and (22) were utilised for the derivation of the average bond stress according to Eurocode 2 [43] and *fib* Model Code [38], respectively, which is given in Table 2. Considering the upper and lower values as defined in Eq. (18) for the definition of the height of the tension zone in the core component of the composite cross section, ℓ_c, leads to the estimation of s_r = (313~551) mm for Eurocode 2 [48] and s_r = (397~698) mm for the *fib* Model Code [38]. It is seen that the Model Code model for the average bond stress yields higher values for the bond stress of plain bars and lower values for the bond stress of the ribbed bars compared to the corresponding EC2 model [48]. The analyses conducted with the solution algorithm considered a natural interface corresponding to a friction coefficient μ=0.4 according to the Greek code for interventions [14]. Axial load was applied to the core of the composite cross section following the experimental setup, and slip was allowed at the interfaces between the existing cross section and the jacket. The response of the QRC specimen in terms of monotonic moment – curvature relationships for the various definitions of crack spacing is shown in Fig. 11 along with the experimental hysteresis loops. The comparison was based on the use of monotonic response curves (envelope curves of the hysteresis loops for null degradation, α=1), with a view to avoiding any further complexity due to the cyclic loading conditions (i.e. influence of degradation rules on response). As shown in Fig. 11, the curve derived for a crack spacing estimation equal to s_r = 551 mm using the Eurocode 2 [48] expression for the upper limit of ℓ_c (=400-118-75 = 207 mm, see Table 2), the red coloured curve, reasonably matches the strength and stiffness level of the experimental curve up to the peak strength value. The use of the lower value for ℓ_c leads to response curves that underestimate the actual response irrespective of the code expression used. It is thus concluded that the Eurocode 2 [48] expression for estimating the average bond stress may be

considered adequate when the height of the tension zone in the core component of the composite cross section, ℓ_c, is taken equal to the upper limit value defined in Eq. (18).

Table 1: Reinforcement detailing and material properties of the test data of Bousias et al. [9].

Specimen	Long. Reinf.	Stirrups original	$f_{c,c}$ (MPa)	$f_{y,c}$ (MPa)	$f_{yw,c}$ (MPa)	Long. Reinf.	Stirrups jacket	$f_{c,J}$ (MPa)	$f_{y,J}$ (MPa)	$f_{yw,J}$ (MPa)
QRC	4Ø14	Ø8/200	26.3	313	425	4Ø20	Ø10/100	55.3	487	599
QRCR	4Ø14	Ø8/200	27.7	313	425	4Ø20	Ø10/100	55.3	487	599
QRCD	4Ø14	Ø8/200	27.4	313	425	4Ø20	Ø10/100	55.3	487	599
QRCRD	4Ø14	Ø8/200	26.3	313	425	4Ø20	Ø10/100	53.2	487	599
QRCW	4Ø14	Ø8/200	22.9	313	425	4Ø20	Ø10/100	28.7	487	599
QRCM	-	-	30.6	-	-	4Ø20	Ø10/100	-	487	599

Table 2: Estimation of crack spacing, s_r.

Code	$f_{ctm,c}$ (MPa)	$f_{ctm,J}$ (MPa)	$f_{b,c}$ (MPa)	$f_{b,J}$ (MPa)	ℓ_c (mm)	s_r (mm)
Eurocode 2	2.65	4.35	2.65	9.80	207	551
					75	313
fib Model Code	2.65	4.35	3.09	7.03	207	698
					75	397

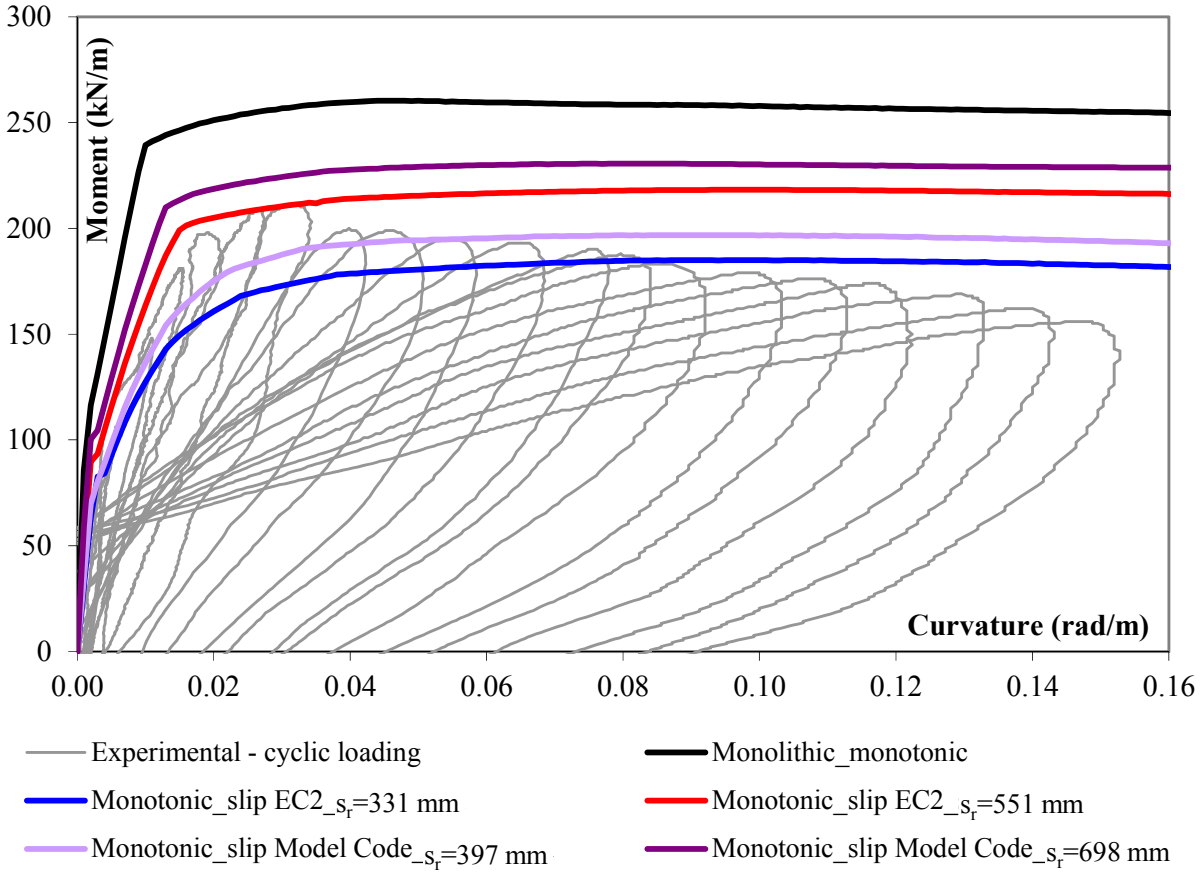

Figure 11: Comparison of the moment – curvature response curves derived for the various crack spacing estimations with the experimental moment – curvature hysteresis loops.

4.2 Effect of cyclic degradation

The sensitivity of the proposed model to the degradation rules adopted from the Greek code for interventions, KANEPE [14] (Eqs. (5, 8)), as modified for the needs of the present study (Eqs. (9-13)) was examined. To this purpose, specimen QRC with the details given in the previous paragraph was utilised for carrying out cyclic loading analyses with degradation parameter α assuming values from 0.1 to 1, with a step of 0.1. The directional degradation effect was ignored in these analyses since its influence on response is examined separately in the next section. The comparison of the resulting response curves for the various α values, revealed that the value of $\alpha = 1$ suggested by the Greek code for interventions [14] leads to underestimation of the actual response as provided by the experimental hysteretic curves (Fig. 12(a)). However, a value of $\alpha = 0.5$ seems to yield hysteretic curves that correlate well with

the experimental ones (Fig. 12(b)). It is concluded that the degradation rules adopted by the Greek code for interventions [14] are rather conservative (which is not surprising for a code of practice) and by employing lower values for degradation factor α (Eqs. (12, 13) the derived hysteretic curves match the experimental ones.

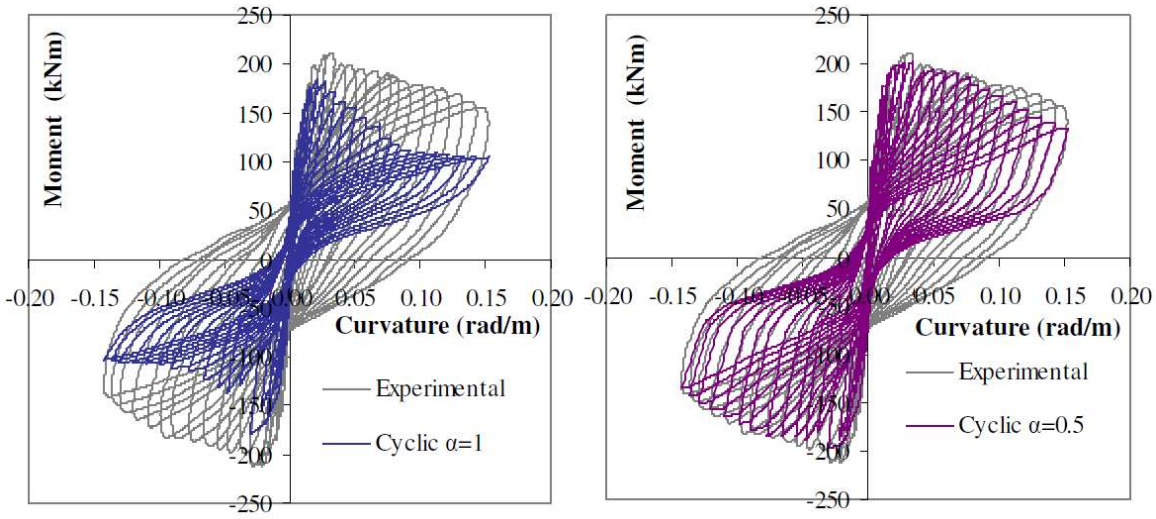

Figure 12: Comparison of moment – curvature response histories for α=1 and α=0.5 with experimental data.

4.3 Influence of directional degradation

Another parameter that has not been investigated so far is the directional degradation of the shear resistance mechanisms (Eqs. 9 and 10). The moment – curvature response history for QRC for $\alpha = 0.5$ and adopting the proposed directional degradation rules appears in Fig. 13. If compared with Fig. 12(b), it is clear that directional degradation leads to underestimation of the actual response as provided by the experimental hysteretic curves, which is more pronounced in the negative direction of loading. Thus, based on this observation it was decided to exclude directional degradation from further analyses.

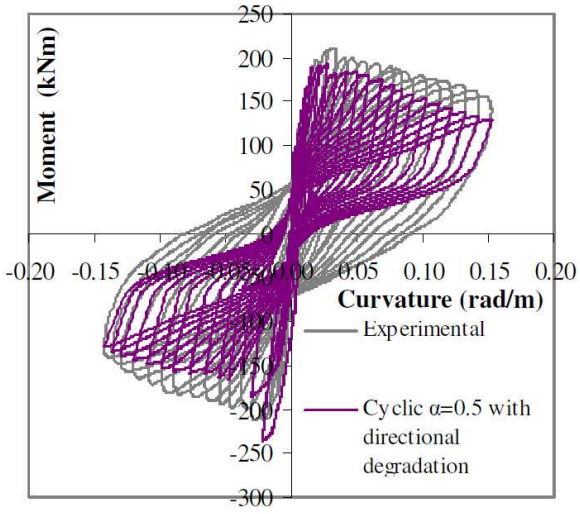

Figure 13: The influence of directional degradation on the moment – curvature response histories for α=0.5.

5. Experimental validation

The validity of the proposed analytical model for predicting the flexural response of RC jacketed members under cyclic loading was examined by comparing the moment – curvature histories derived by the analytical model with those for the specimens studied by Bousias *et al.* [10]. The decision to select this experimental study was based not only on its scope, but also on the fact that it provides detailed test results in terms of moment – curvature curves.

All specimens had the same geometry and the same jacket thickness as specimen QRC described in the previous section (more details can be found in the paper describing the database compiled by Thermou *et al.* [12]). Specimen QRCM was a control specimen built monolithically having the same geometry as the jacketed members, its only longitudinal reinforcement being that of the jacket. Apart from specimen QRC for which no special measures were taken to connect the existing member to the jacket, for all other specimens various connection measures were examined. In specimen QRCR, the full lateral surface of the existing column was roughened using a pneumatic chipping device, and in QRCD three 16 mm dowels were driven into each side of the existing column, at distances of 200, 650, and 1100 mm from the top of the footing. In QRCRD the measures taken in QRCR and QRCD

were combined. In QRCW the corner bars of the jacket were connected to the corresponding existing ones by welding both of them to 16 mm diameter, 400 mm long deformed reinforcing bars bent into a U-shape.

The estimation of the crack spacing is presented in Table 3 following the outcome of the preceding sensitivity study. The proposed analytical model took into account the various alternative connection measures applied in the specimens tested by Bousias *et al.* [10]. Different values for the friction coefficient, μ, were utilised to reflect the roughness of the interface. For those specimens with a smooth surface (QRC, QRCW) the friction coefficient assumed a value of $\mu = 0.4$. In the case of specimens wherein the full lateral surface of the existing column was roughened (QRCR, QRCRD) the friction coefficient μ assumed a value of 0.8 that falls within the range of values proposed for a rough interface by the *fib* Model Code [38]. The dowels placed to strengthen the connection between the old and new member were also modelled. Moreover, in the case of specimen QRCW, the U-shape links used to connect the existing longitudinal reinforcement to the new longitudinal reinforcement of the jacket were modelled through an equivalent number of dowels.

Table 3: Estimation of crack spacing, s_r.

Specimen	QRC	QRCR	QRCD	QRCRD	QRCW
$f_{ct,c}$ (MPa)	2.65	2.75	2.75	2.65	2.42
$f_{ct,J}$ (MPa)	4.35	4.35	4.35	4.24	2.81
$f_{b,c}$ (MPa)	2.65	2.75	2.75	2.65	2.42
$f_{b,J}$ (MPa)	9.80	9.80	9.80	9.55	6.33
ℓ_c (mm)	207	203	205	203	204
s_r (mm)	551	547	550	546	583

The comparison between the experimental and the analytical moment – curvature histories are presented in Fig. 14. In the monolithic specimen, QRCM, the response of the analytical model (it is noted that no slip takes place at the interface since a monolithic cross section is

considered) matches the secant stiffness at yield, maximum strength and pinching of the hysteresis loops, but fails to follow the strength degradation for curvature values higher than 0.05 rad/m. The moment – curvature hysteretic curves for specimens QRC, QRCR, QRCD, QRCRD and QRW were estimated utilising the analytical model, adopting $\alpha = 0.5$ (Eqs. 12, 13) based on the preceding sensitivity study. It is observed that the analytical curves reasonably match the strength and stiffness level of the experimental curves at each loading step. When slip is taken into account, pinching is more pronounced in the analytical model, indicating less energy dissipation at each loading cycle, which is an indication of conservatism. The comparative results of Fig. 14 indicate that irrespective of the connection measures taken, a common value for degradation factor α appears to be suitable. This may be justified by the observation made by Bousias *et al.* [10] that the key properties such as yield moment, yield drift, secant stiffness at incipient yielding, and flexure-controlled ultimate drift, do not systematically depend on the type of connection measures taken. An exception to this observation refers to the ultimate chord rotation which increased by approximately 16% when the connection measures are dowels or U-bars welded between the new and the existing longitudinal bars.

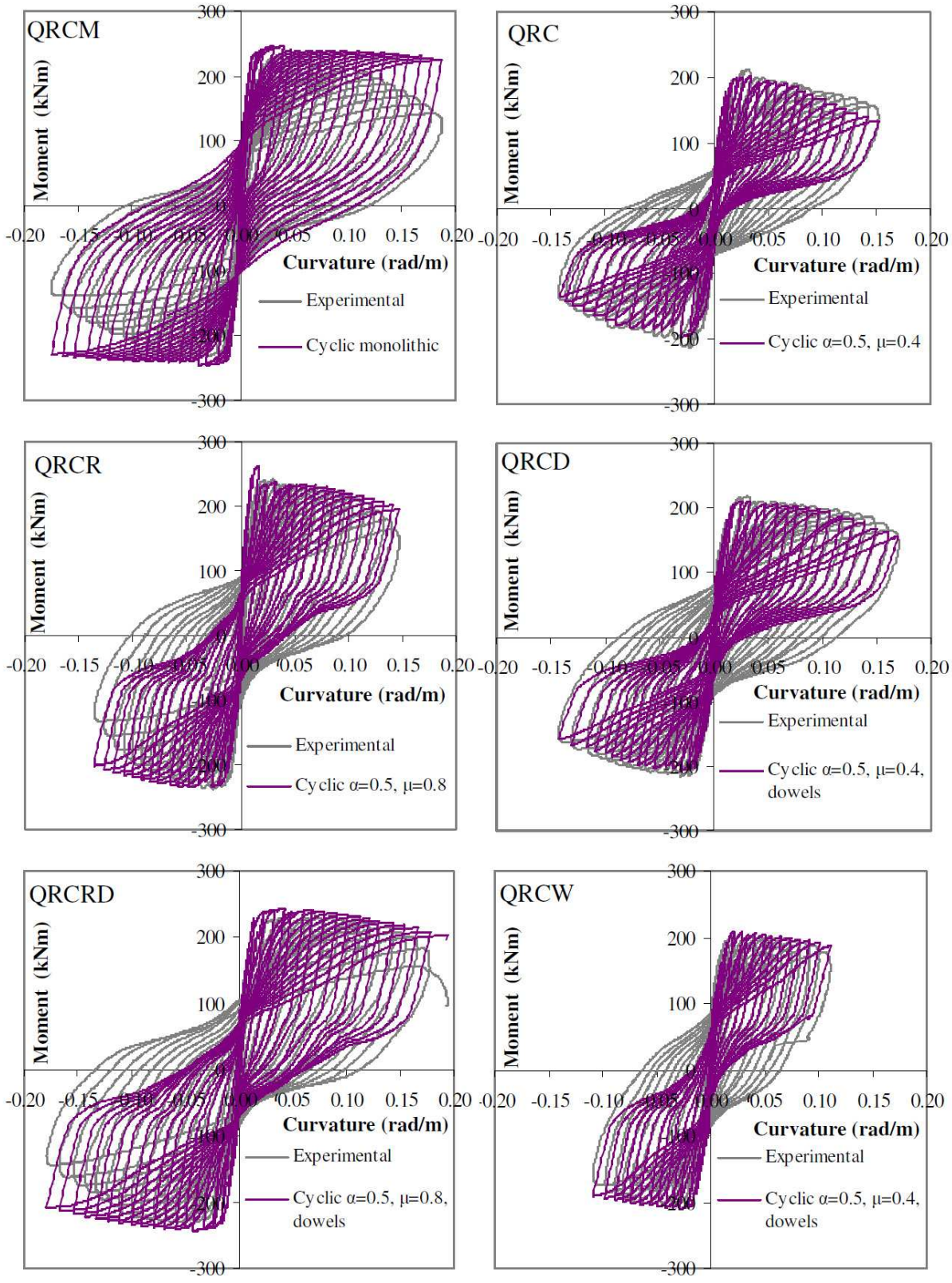

Figure 14: Comparison of moment – curvature response histories for α=0.5 with directional degradation with the corresponding experimental ones.

6. Conclusions

The response under reversed cyclic loading of old-type RC columns strengthened through concrete jacketing was studied herein. In the proposed analytical model partial connection between the core and the jacket are assumed, while slip can take place at the interfaces. The composite cross section is divided into three layers which develop the same curvature. The interface characteristics play a crucial role in the response of the composite member. The proposed algorithm aims at establishing equilibrium at both interfaces, which is achieved when shear capacity equals shear demand at each curvature loading step. Shear capacity at each loading step is described by existing constitutive models for cyclic loading conditions, which are further modified and enhanced for the needs of the present research. Shear demand at the interfaces is estimated by considering the flexural stresses on each layer of the cross section and is controlled by the distance between successive cracks. A sensitivity study was conducted to investigate the impact of crack spacing and degradation rules on the moment - curvature response curves. It was shown that adopting the average bond stress model as proposed by EC2 [39] and considering the height of the tension zone in the core of the composite cross section, ℓ_c equal to the upper limit defined by Eq. (18), the estimated crack spacing, s_r, leads to moment – curvature response curves that correlate well with the experimental data. Moreover, a reduced degradation factor, α=0.5, leads to analytical moment – curvature histories that match reasonably closely the experimental data. The analytical model was implemented for the derivation of the moment – curvature histories of a group of test specimens where different connection measures were taken. The derived analytical curves reasonably matched the experimental ones, thus manifesting the validity of the proposed analytical model for RC jacketed members under cyclic loading. Nevertheless, when slip is taken into account, the effect of pinching is more pronounced in the analytical model,

indicating less energy dissipation at each loading cycle, which is conservative, but also indicates a need for future improvement of the rules affecting pinching.

Acknowledgements

The research reported herein was funded by the Greek Earthquake Planning and Protection Organization (EPPO); this support is gratefully acknowledged. Experimental data regarding moment-curvature histories for comparative evaluation of the analytical model were kindly provided by Prof. S.N. Bousias (Patras University).

References

[1] Rodriguez M, Park R. Seismic load tests on reinforced concrete columns strengthened by jacketing. ACI Struct J. 1994;91(2): 150-159.

[2] Gomes AM, Appleton J. Repair and strengthening of RC elements under cyclic loading. In: Proceedings 11th European Conference on Earthquake Engineering, A.A. Balkema (Rotterdam, The Netherlands), Paris, France, 1998.

[3] Ilki A, Darilmaz K, Bakan I, Zorbozan M, Yuksel E, Haruhan S, Karadogan F. Jacketing of prefabricated columns. In: 2nd Japan-Turkey Workshop on Earthquake Engineering, 1998; 329-336, Istanbul, Turkey.

[4] Vandoros KG, Dritsos SE. Interface treatment in shotcrete jacketing of reinforced concrete columns to improve seismic performance. J. Struct Eng and Mech 2006;23(1): 43-61.

[5] Vandoros KG, Dritsos SE. Axial preloading effects when reinforced concrete columns are strengthened by concrete. Progr in Struct Eng and Mat J. 2006;8(3): 79-92.

[6] Vandoros KG, Dritsos SE. Concrete jacket construction detail effectiveness when strengthening RC columns. Constr Build Mater 2008;22: 264-276.

[7] Júlio ENBS, Branco FAB, Silva VD. Reinforced concrete jacketing - Interface influence on monotonic loading response. ACI Struct J 2005;102(2): 252-257.

[8] Bousias S, Spathis A.-L, Fardis MN. Concrete or FRP jacketing of columns with lap splices for seismic rehabilitation. J. Adv Concr Tech 2006;4(3): 431-444.

[9] Bousias S, Biskinis D, Fardis MN, Spathis A-L. Strength, stiffness, and cyclic deformation capacity of the concrete jacketed members. ACI Struct J 2007;104(5): 521-531.

[10] Bousias S, Spathis A-L, Fardis MN. Seismic retrofitting of columns with lap-spliced smooth bars through FRP or Concrete Jackets. J Earthq Eng 2007;11: 653-674.

[11] Júlio ENBS, Branco FAB. Reinforced concrete jacketing - Interface influence on cyclic loading response. ACI Struct J 2008;105(4): 417-477.

[12] Thermou GE, Papanikolaou VK, Kappos AJ. Analytical model for predicting the response of old-type columns rehabilitated with concrete jacketing under reversed cyclic loading. In: ECCOMAS Thematic Conference "Computational Methods in Structural Dynamics and Earthquake Engineering (COMPDYN 2011), Corfu, Greece, 2011; Paper No CD 137.

[13] Eurocode 8, Design of structures for earthquake resistance - Part 1: general rules, seismic actions and rules for buildings. EN1998-1-2004:E, European Committee for Standardization (CEN), Brussels, 2004.

[14] Greek Code for Interventions (KANEPE). Earthquake Planning and Protection Organization, Athens, 2013.

[15] Lampropoulos AP, Dritsos SE. Modelling of RC columns strengthened with RC jackets. Earthquake Engng Struct Dyn. 2011; 40:1689–1705.

[16] Lampropoulos AP, Dritsos SE. Concrete shrinkage effect on the behavior of RC columns under monotonic and cyclic loading. Construction and Building Materials 2011; 25: 1596-1602.

[17] Thermou GE, Pantazopoulou SJ, Elnashai AS. Flexural behavior of brittle RC members rehabilitated with concrete jacketing. J Structural Engineering 2007;133(10):1373-1384.

[18] Choi D-U, Fowler DW, Jirsa JO. Interface shear strength of concrete at early ages. ACI Struct J 1999;96(3): 343-348.

[19] Júlio ENBS, Branco FAB, Silva VD. Concrete-to-concrete bond strength - Influence of the roughness of the substrate. Constr Build Mater 2004;18: 675–681.

[20] Júlio ENBS, Branco FAB, Silva VD, Lourenco JF. Influence of added concrete compressive strength on adhesion to an existing concrete substrate. Build Environ 2006;41: 1934–1939

[21] Santos PMD, Júlio ENBS. Factors affecting bond between new and old concrete. ACI Mater J 2011;108(4): 449-456.

[22] Santos PMD, Júlio ENBS. Interface shear transfer on composite concrete members. ACI Struct J. 2014; 111(1): 113-121.

[23] Birkeland PW, Birkeland HW. Connections in precast concrete construction. J ACI 1966;63(3): 345-368.

[24] Walraven JC. Fundamental analysis of aggregate interlock. Struct. Div. ASCE 1981;107(ST11): 2245-2270.

[25] Loov ER, Patnaik KA. Horizontal shear strength of composite concrete beams with a rough interface. PCI J 1994: 48-69.

[26] ACI Committee 318. Building Code Requirements for Reinforced Concrete (ACI 318-02) and Commentary ACI 318 R-02. American Concrete Institute, Detroit, 2002: 139–154.

[27] Climaco JCTS, Regan PE. Evaluation of bond strength between old and new concrete in structural repairs. Mag Concr Res 2001;53(6): 377-390.

[28] Mattock HA, Hawkins MN. Shear transfer in reinforced concrete- recent research. PCI J 1972: 55-75.

[29] Mattock HA, Li KW, Wang CT. Shear transfer in lightweight reinforced concrete. PCI J. 1976: 20-39.

[30] Mattock HA. Shear friction and high-strength concrete. *ACI Struct. J* 2001;98(1): 50-59.

[31] Vecchio FJ, Collins MP. The modified compression field theory for reinforced concrete elements subjected to shear. J ACI 1986; 83(2): 219-231

[32] Tassios TS. Fundamental mechanisms of force-transfer across reinforced concrete critical interfaces. In: CEB Workshop, West Germany, 1986; 381-397.

[33] Vassilopoulou I, Tassios P. Shear transfer capacity along a RC crack under cyclic sliding. In: Proceedings fib Symposium, Technical Chamber of Greece, Athens, Greece 2003;Paper No. 271.

[34] Tassios T, Vintzileou E, Concrete-to-concrete friction. ASCE J. Struct. Eng. 1987; 113(4): 832-849.

[35] Vintzileou E, Tassios TS. Mathematical models for dowel action under monotonic and cyclic conditions. Mag Concr Res 1986; 38(134):13-22.

[36] Vintzileou E, Tassios TS. Behavior of dowels under cyclic deformations. ACI Struct J 1987;84(1):18-30.

[37] Palieraki V, Vintzileou E, Zeris C. Behaviour of interfaces in repaired/strengthened RC elements subjected to cyclic actions: Experiments and Modelling. In: 3rd international symposium on life-cycle and sustainability of civil infrastructure systems (IALCCE'12), Vienna, Austria, 2012.

[38] *fib* Model Code for Concrete Structures 2010. Ernst & Sohn; 2013.

[39] Kaklauskas G, Gribniak V, Bacinskas D, Vainiunas P. Shrinkage influence on tension stiffening in concrete members. Eng Struct 2009; 31(6): 1305–12.

[40] Mander JB, Priestley MJN, Park R. Theoretical stress-strain model for confined concrete. Journal of Structural Engineering 1988; 114(8): 1804-1826.

[41] Martinez-Rueda JE, Elnashai AS. Confined concrete model under cyclic load. Materials and Structures 1997; 30(3): 139-147.

[42] Menegotto M, Pinto PE. Method of analysis for cyclically loaded RC plane frames including changes in geometry and nonelastic behaviour of elements under combined normal force and bending. Proc. IABSE Symposium, 1973, Lisbon, Portugal.

[43] Filippou FC, Popov EP, Bertero VV. Effects of bond deterioration on hysteretic behaviour of reinforced concrete joints. Report No. UCB/EERC-83/19 1983, University of California, Berkeley.

[44] Papanikolaou VK, Stefaniou SP, Kappos AJ. The effect of preloading on the strength of jacketed R/C columns. Construction and Building Materials 2013: 38: 54–63.

[45] Bonet JL, Romero ML, Miguel PF, Fernandez MA. A fast stress integration algorithm for reinforced concrete sections with axial loads and biaxial bending. Comp Struct 2004;82(2-3): 213-225.

[46] Kappos AJ. Analytical prediction of the collapse earthquake for RC buildings: Suggested methodology. Earthq Eng Struct Dyn 1991; 20(2): 167-176.

[47] Storn R, Price K. Differential Evolution – A simple and efficient heuristic for global optimization over continuous spaces. J Glob Opt 1997; 11(4): 341-359.

[48] Eurocode 2. Design of concrete structures – Part 1-1: General rules and rules for buildings. EN 1992-1-1:2004. European Committee for Standardization (CEN), Brussels, 2004.

[49] Greek Seismic Code. Earthquake and Planning Protection Organization, Athens; 2000.